Hindawi
Shock and Vibration
Volume 2023, Article ID 2731176, 12 pages
https://doi.org/10.1155/2023/2731176

Research Article

Squeeze Film Effect and Its Influence on the Lubrication Characteristics of Slipper Oil Film under Pressure Pulse

JiaHao Wu, LiFeng Ma, GaoCheng An, and Hao Han

College of Mechanical Engineering, Taiyuan University of Science and Technology, Taiyuan 030024, Shanxi, China

Correspondence should be addressed to LiFeng Ma; mlf_zgtyust@163.com

Received 17 January 2022; Revised 16 March 2022; Accepted 12 April 2022; Published 7 June 2023

Academic Editor: Arturo Garcia-Perez

This study aims at the lubricant film between the slipper and swashplate of an axial piston pump. Based on a single piston/slipper assembly model, a mathematical model for the squeeze film effect is developed according to the pressure-flow transfer process as well as the dynamics of the piston/slipper assembly. The squeeze film effect on the slipper lubricant film has been predicted by nonlinear numerical calculations and computational fluid dynamic (CFD). The slipper lubricant film thickness and leakage flow, sealing land pressure distribution, and load carrying capacity are evaluated as important parameters to indicate the performance of slipper oil film. The influence of piston/slipper assembly geometric parameters, oil compressibility, and oil viscosity on the squeeze film effect under pressure pulse has been studied, and the effect of squeeze film speed on the support force of slipper lubricant film has been given out.

1. Introduction

In the process of diversified and extreme applications of axial piston pumps, the performance requirements of the key friction pairs are becoming higher and higher, and the slipper-swashplate pair is one of the key friction pair of axial piston pumps, which is most prone to wear and thus affects the reliability of the piston pumps. During the operation of an axial piston pump, a micrometer-thick oil film exists between the slipper and swashplate, which plays the role of lubrication and support and is the key to protect the friction pair to avoid wear. When its load carrying capacity is not enough to resist the external load force, the slipper friction pair will be in the extreme working condition of boundary lubrication or even dry friction, and the surface of the slipper or swashplate will wear quickly, causing the pump to fail to operate properly. The oil film lubrication characteristics of the slipper directly affect the working performance of the piston pump. The study on the oil film of the slipper and the squeeze film effect on the performance has an important guiding significance for the structural design of the axial piston pump.

Many theoretical analyses and experimental research studies on the fluid lubrication characteristics between the slipper and swashplate of axial piston pump have been continuously explored in recent years. Canbulut [1] used experimental measurements to investigate the impact of surface roughness, damping orifice, pressure in the piston chamber, and rotation speed on the leakage flow of the slipper-swashplate pair under the hydrostatic support, but these experiments did not show the characteristics of the lubricant film between slipper and swashplate at the moment of the pressure pulse in the piston chamber. Harris et al. [2] developed a numerical model to predict the lift and tilt behavior of the slipper-swashplate pair under a constant temperature field. They investigated and verified by experiments that the load and overturning characteristics of the slipper may lead to contact between slipper and swashplate. However, the squeezing film effect was not considered. Deeken [3–5] analyzed the oil film characteristics of the slipper pair in a hydraulic pump by virtual prototype simulation and verified the simulation results through experiments. Manring et al. [6] studied the influence of different ball and socket structures of slipper on the oil film

characteristics of slipper pairs through experiments. Borghi et al. [7] established a static model of slipper to predict the critical speed of excessive increase of the oil film thickness between the slipper and swashplate and paid attention to the influence of spring pressure on the maximum rotation speed of the pump. In this model, the pressure change of the piston chamber and the viscous friction of the piston pair were considered. Hooke et al. [8, 9] have studied the effects of the oil conditions and slipper surface conditions on the performance of slipper and measured the oil film thickness in a short time during the operation of the piston pump. They have conceived that in the slipper structure designed according to the hydrostatic bearing method, the compression force of the slipper is not only provided by the hydrostatic supporting force but also balanced by the dynamic pressure effect of the oil film between the slipper and the swashplate. And they compared the bearing capacity of the slipper pair under different damping orifices through experiments and verified the balance performance of the slipper pair under different static pressure effect designs. The Ivantysynova and Huang [10] team coupled the dynamic characteristics of the slipper with the multiphysical field and obtained more accurate results than with the single physical field. The CASPAR software program was compiled to study the hydrodynamic, dynamic, and temperature characteristics, and the viscosity, temperature, and pressure of the oil and the compressibility of the oil were considered. Schenk [11] established a new model of slipper pair, used this to solve the dynamic pressure field and thickness field of slipper pair during operation, and verified the working characteristics of the oil film of slipper pair by displacement sensor. Zhang et al. [12, 13] studied the spin motion of axial piston pump slippers through experiments; they used sensors to measure the spin speed of the slipper while the pump was operating, they also used sensors and other means to measure the thickness of the slipper oil film at multiple points and they obtained some experimental sample data. A theoretical study has been studied the effect of surface roughness on the hydrodynamic lubrication of squeeze film between a sphere and a flat plate by Naduvinamani et al. [14]. It is found that azimuthal roughness could increase the load carrying capacity and squeeze film time compared to smooth condition. Qing-rui and Hou [15] have investigated the squeeze film effect on hydro-viscous drive speed regulation and obtained an approximate 30% increase in oil film loading capacity for the squeeze film effect. They also found that the squeeze film effect is very slight in the early stages of the startup process, but the squeeze film effect becomes more and more remarkable as the oil film thickness decreases in the later stages. The negative offset surface roughness pattern was found to increase the load carrying capacity and oil film squeeze time through numerical analysis by Bujurke et al. [16]. Walicka [17] has obtained the pressure distribution of the Schulman fluid squeeze oil film effect on porous surfaces by a continuous approximation method. Haidak and Wang [18] realized the damage and fatigue analysis of the slipper/swashplate interface by predicting the solid deformation, strain, and wear of the solid for a given material. Ye et al. [19, 20] studied the bearing capacity of the surface-textured slipper, introduced the elastohydrodynamic lubrication model, analyzed the bearing capacity of the oil film of the slipper pair under different speeds and load pressures and considered the comprehensive effects of inclination angle, area density, depth diameter ratio, and other factors. In addition, they also established the thermal elastohydrodynamic lubrication model of the slipper oil film for the piston pump and discussed the deformation of the slipper and the distribution of slipper oil film thickness, pressure, and temperature. The effects of working conditions and structural parameters of slippers, such as oil film thickness, pressure, temperature and leakage flow, on the lubrication performance of TEHD are studied, and the experiments show that this research has certain guiding significance for the structural optimization of slippers. Based on the equation of motion, generalized Reynolds equation, energy equation, and Fourier heat equation, Hashemi et al. [21] established the multibody dynamics calculation model of a swashplate axial piston pump and discussed the influence of the holding device on slipper friction and temperature.

The squeeze film phenomenon exists between the slipper and swashplate of an axial piston pump, as these two lubricating surfaces are near each other at a high speed during the pump operation. This study focuses on the squeeze film effect at the sliding interface between the slipper and swashplate. To further predict the squeeze effect on the lubricant film, a numerical model will be developed. The numerical model of the squeeze film effect considers the multiphysics and multiscale, and it can predict the squeeze film effect under the pressure pulse. Figure 1 shows the axial piston pump and its component parts.

2. Mathematical Model

In this section, the mathematical model of the squeeze film effect on slipper lubricant film will be derived from the dynamics of the piston/slipper assembly and the pressure-flow transfer of fluid. We can predict the force and motion trend of the piston/slipper assembly based on the dynamics model under the squeeze film effect. At the same time, we can predict the pressure distribution and flow transfer on the slipper oil film under the squeeze film effect according to the fluid lubrication model. In order to simplify the model, only the hydrostatic nature of the fluid is considered.

2.1. Dynamics Model of the Piston/Slipper Assembly. Figure 2 gives the external forces acting on the piston/slipper assembly. The assembly is balanced by compression force and support force. The compression force contains F_p, F_k, F_a, F_f, where F_p is the hydraulic force caused by oil pressure from the displacement chamber, F_k is the spring force, F_a is the inertia force due to the movement of the piston/slipper assembly, F_f is the friction force caused by friction reaction of the cylinder bore. In this paper, the support force generated by the lubricant film between slipper and swashplate is divided into hydrostatic support force F_{N1} and the squeeze support force F_{N2}. These support forces play a role of the lifting the piston/slipper assembly.

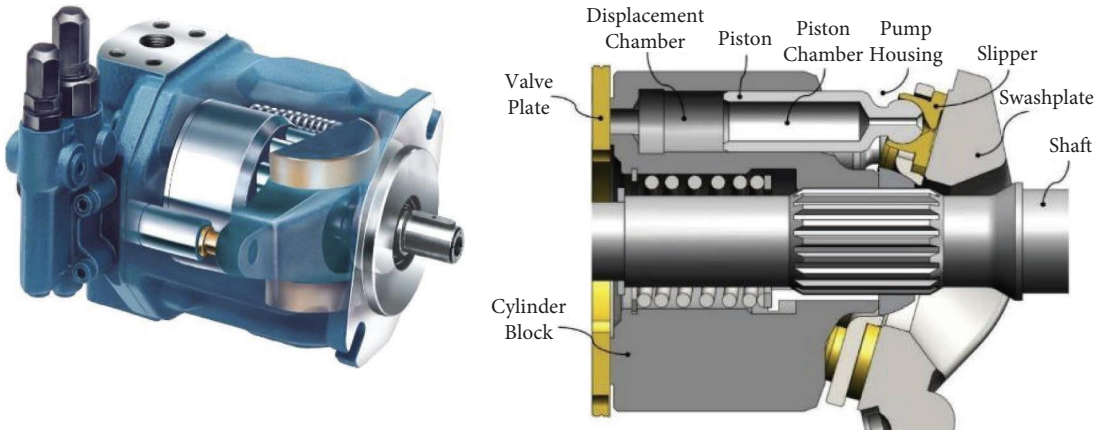

Figure 1: Axial piston pump and its component parts.

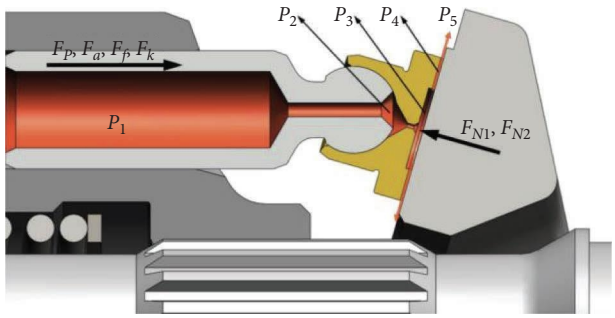

Figure 2: External forces acted on a single piston/slipper assembly.

In the process of modeling squeeze film effect, only the oil pressure from the bottom of the piston is considered, as the other forces only affect the value of the compression force. They have no influence on the analysis of the squeeze film effect. Thus, the force balance equation of the piston/slipper assembly parallel to direction of the shaft axis can be written as follows:

$$F_p - (F_{N1} + F_{N2}) \cos\theta = \mathrm{ma}, \tag{1}$$

where the hydraulic force can be given by

$$F_p = \pi r_1^2 p_1. \tag{2}$$

2.2. Hydrostatic Support Force. Due to differential pressure at the inlet and outlet of the slipper sealing land, a hydrostatic support force exists on the sealing land between the slipper and swashplate. The pressure drop causes oil to flow from the slipper pocket to the pump chamber, creating a pressure distribution on the sealing land. Figure 3 shows the schematic diagram of the slipper pair.

The support forces resulting from pressure distribution on the sealing land of the slipper [22] can be described as follows:

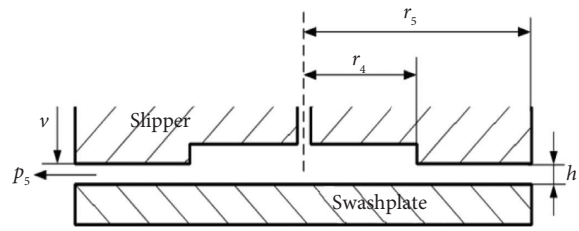

Figure 3: Schematic diagram of the slipper pair.

$$F_{N1} = \frac{\pi}{2}\left[\frac{r_5^2 - r_4^2}{\ln(r_5/r_4)}\right] p_3. \tag{3}$$

According to the abovementioned equation, the hydrostatic support force on the sealing land of the slipper is influenced by the geometric parameters of the slipper, independent of the film thickness.

2.3. Support Force from the Squeeze Film Effect. As shown in Figure 2, during operation of the hydraulic pump, a lubrication oil film of thickness h is formed between the slipper and swashplate. The piston continuously suctions and discharges the pressure at the bottom of the piston constantly switches. Then the oil film of the slipper is squeezed and thinned at a speed v. Meanwhile, there is a certain amount of flow to be excluded along the circle to the piston chamber. Then the squeeze film effect produces a pressure field, which means the squeeze film effect produces a support force.

The microelementary ring at radius of r is used as an object to study.

Under the effect of pressure drop, the flow through this microelement ring band is presented as follows:

$$q = -\frac{\pi r h^s}{6\mu} \frac{\mathrm{d}p}{\mathrm{d}r}. \tag{4}$$

Similarly, the pressure distribution [22] along the radius is as follows:

$$p = \frac{3\mu}{h^3}\frac{\mathrm{d}h}{\mathrm{d}t}\left[\left(r^2 - r_4^2\right) - \left(r_5^2 - r_4^2\right)\frac{\ln\left(r/r_4\right)}{\ln\left(r_5/r_4\right)}\right]. \quad (5)$$

The support force formed by the squeeze film effect can be expressed as follows:

$$F_{N2} = -\frac{3\pi\mu}{2h^3}\frac{\mathrm{d}h}{\mathrm{d}t}\left[r_5^4 - r_4^4 - \frac{\left(r_5^2 - r_4^2\right)^2}{\ln\left(r_5/r_4\right)}\right]. \quad (6)$$

The dynamics of piston/slipper assembly under the squeeze film effect is modeled as follows:

$$\begin{aligned} \mathrm{ma} = {} & p_1\pi r_1^2 - \frac{\pi}{2}\frac{r_5^2 - r_4^2}{\ln\left(r_5/r_4\right)}p_3\cos\theta \\ & - \frac{3\pi\mu}{2h^3}\frac{\mathrm{dh}}{\mathrm{dt}}\left[\left(r_5^4 - r_4^4\right) - \frac{\left(r_5^2 - r_4^2\right)^2}{\ln\left(r_5/r_4\right)}\right]\cos\theta. \end{aligned} \quad (7)$$

2.4. Fluid Lubrication Model of Slipper Pads under the Squeeze Film Effect. As shown in Figure 4, oil from the piston chamber flows through the piston orifice into the slipper socket, then through the slipper orifice into the slipper pocket, and finally through the gap between the slipper and swashplate into the pump chamber. A layer of lubricating oil film is formed between the slipper and swashplate.

The pressure-flow transfer process in the piston/slipper assembly is analyzed, and then a fluid lubrication theoretical model of the slipper lubricant film under squeeze film effect is instituted.

The following assumptions were made:

(1) Neglecting the effects of surface tolerances, slipper and swashplate defects, and surface structure on oil film properties

(2) Disregarding the dynamic pressure effect on the oil film of the slipper, it is considered that the bottom surface of the slipper is always parallel to the plane of the swashplate

(3) Leakage at the slipper socket is not considered

(4) Assume that oil density does not change with temperature.

Oil from the piston chamber passes through the piston orifice to the slipper socket and creates a pressure drop. The flow equation through the piston orifice [22] is as follows:

$$q_1 = \frac{\pi r_2^4}{8\mu l}\left(p_1 - p_2\right). \quad (8)$$

Oil enters the slipper pocket through the slipper orifice, and the flow equation through the slipper orifice [22] can be given by

$$q_2 = C_\mathrm{d}\pi r_3^2\sqrt{\frac{2}{\rho}\left(p_2 - p_3\right)}, \quad (9)$$

where q_1 is equals to q_2; thus,

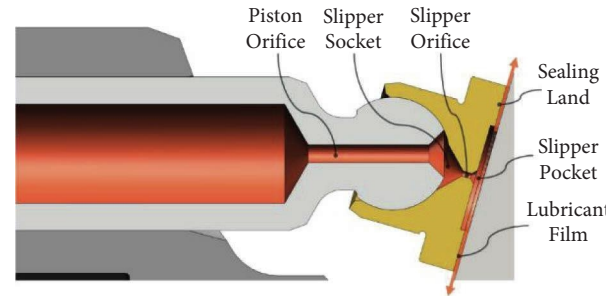

Figure 4: Schematic diagram of the oil control chamber in the piston/slipper assembly.

$$q_1 = \frac{8\pi C_d^2\mu l r_3^4\left(\sqrt{1 + \rho/32r_2^6\left(p_1 - p_3\right)/C_\mathrm{d}^2\mu^2 l^2 r_3^4} - 1\right)}{\rho r_2^4}. \quad (10)$$

Oil from the slipper pocket flows through the gap between slipper and swashplate to the pump chamber, and q_3 can be written as follows:

$$q_3 = \frac{\pi h^3\left(p_3 - p_5\right)}{6\mu\ln\left(r_5/r_4\right)}. \quad (11)$$

The pressure pulse causes a change in force at the bottom of the piston, the force which causes the piston/slipper assembly move towards the swashplate, and then the slipper lubricant film is squeezed. The film thickness decreases due to the squeeze film effect on the slipper. For the expression of equation, we need to make another assumptions, assuming that the initial oil film thickness is h_0, the change of oil film thickness is x, so that, the oil film thickness can be expressed as

$$h = h_0 - x, \quad (12)$$

where the pump chamber pressure is 0, and then equation (11) becomes

$$q_3 = \frac{\pi\left(h_0 - x\right)^3 p_3}{6\mu\ln\left(r_5/r_4\right)}. \quad (13)$$

The flow rate over the sealing land of the slipper can be given by

$$Q_x = q_3 + q_4, \quad (14)$$

where q_4 is the flow produced by the squeeze film effect, q_4 can be given by

$$q_4 = \pi\left(r_5{}^2 - r_4{}^2\right)\frac{\mathrm{d}x}{\mathrm{d}t}. \quad (15)$$

According to the compressibility equation of the slipper pair fluid,

$$\frac{E}{V_1}\int\left(q_1 - q_3 - q_4\right)\mathrm{d}t = \mathrm{d}p_3. \quad (16)$$

q_1, q_3, and q_4 can be integrated in equation (14), and then the fluid lubrication model of slipper under the squeeze film effect is as follows:

$$\frac{\mathrm{d}p_3}{\mathrm{d}t} = \frac{E}{\pi r_4^2 (h_1 + h_0 - x)} \left(\frac{\sqrt{1 + p/32\left(r_2^6 (p_1 - p_3)/C_\mathrm{d}^2 \mu^2 l^2 r_3^4\right)} - 1}{(p/8\pi)\left(r_2^4/C_\mathrm{d}^2 \mu l r_3^4\right)} - \frac{\pi (h_0 - x)^3 p_3}{6\mu \ln\left(r_5/r_4\right)} - \pi\left(r_5^2 - r_4^2\right)\frac{\mathrm{d}x}{\mathrm{d}t} \right). \tag{17}$$

Equations (7) and (17) presented above are the global relationships that may be used to predict the dynamic behavior of the squeeze film effect on the slipper/swashplate pad system. Equation (7) represents the dynamics model of the piston/slipper assembly, while equation (17) expresses the pressure-flow transfer process of slipper oil film under the squeeze film effect. According to equation (17), we can see that the force conditions and motion trends have an impact on the pressure-flow transfer process, while according to equation (7), we can also get that the pressure distribution and flow transfer affect the dynamics model of the piston/slipper assembly. Only when the two models are combined with each other can we better predict the lubrication characteristics of slipper oil films under the squeeze film effect.

3. Nonlinear Model of the Squeeze Film Effect on Simulink

During the operation of the hydraulic piston pump, the pressure at the bottom of the piston is constantly transformed between high and low pressure due to the continuous rotation of the cylinder. When the pressure at the bottom of the piston changes from the low pressure zone to the high pressure zone, the pressure change in the piston chamber is equivalent to creating a pressure pulse at the bottom of the piston. Therefore, the pressure pulse can most directly reflect the lubrication characteristics of the slipper oil film under excitation conditions. Thus, in the Simulink model, we used the pressure pulse function to research the squeeze film effect, and also in the subsequent study of the fluid field properties, we applied the squeeze film effect under the action of the pressure pulse.

Simulink is used to model the theoretical model of the squeeze film process and analyze the effect of parameter variation on the squeeze film process of the slipper pair. And the Simulink model is shown in Figure 5. The pressure pulse at the bottom of the piston is simulated by using the step function, and 28 MPa is taken.

According to the model, the squeeze film effect with different geometric parameters and different oil viscosities will be studied. Before that, the initial values of the parameters were obtained, and they are listed in Table 1. The different geometric parameters and oil viscosity are selected as a single variable to calculate the model. In order to reveal the properties of lubricant film, the slipper pocket pressure, lubricant film thickness, and leakage will be used to analyze the performance of lubricant film.

From Figure 6(a) and Table 2, under the pressure pulse of 28 MPa, as the r_2 (mm) increases (from 0.6 to 1.2), the slipper pocket pressure increases (from 27.81 MPa to 27.98 MPa), but it takes less time for the slipper pocket pressure to build up (from 6×10^{-5} s to 5×10^{-6} s). These can reveal that as the radius of the piston orifice increases, the damping effect weakens and the response time for pressure buildup continues to decrease. According to Figure 6(b) and Table 2, the time for the slipper pocket pressure to build up increase (from 3×10^{-6} s to 8×10^{-6} s) when the r_3 (mm) increases (from 0.2 to 0.5) and the change of the slipper pocket pressure is no longer significant. For Figure 6(c) and Table 2, when the r_5 (mm) increases (from 12 to 13.5), the slipper pocket pressure decreases (from 27.99 MPa to 27.98 MPa). Although this impact on the pressure value is slight, the effect on the time needed for pressure buildup is remarkable. And the time decreases (from 5×10^{-4} s to 2×10^{-5} s). Meanwhile, r_5 can represent the width of the slipper sealing land. The increase in the width of slipper sealing land leads to an increase in the time required of slipper pocket pressure. Figure 6(d) and Table 2 show that (a) under the pressure pulse of 28 MPa, the slipper pocket pressure increases (from 27.97 MPa to 27.975 MPa) when the h_1 (mm) increases (from 0.5 to 2); (b) the time for slipper pocket pressure to build up increases (from 1×10^{-5} s to 2×10^{-5} s). In fact, h_1 can reflect the volume of the slipper pocket. This numerical model of the squeeze film effect considers the oil compressibility, so we checked the influence of oil compressibility on the pressure buildup of the slipper pocket under the squeeze film effect using the parameter h_1. Figure 6(e) shows the effect of oil viscosity; it has the same trend as Figure 6(c).

Figures 7(a), 7(b), and 7(d) and Table 2 show that (a) the variation of r_2 (mm), r_3 (mm), and h_1 (mm) has almost no influence on the oil film thickness under the squeeze film effect; (b) the lubricant film thickness increases when r_2 increases; (c) the lubricant film thickness decreases while r_3 or h_1 increases. According to Figures 7(c) and 7(e) and Table 1, (a) with the increase of r_5 (mm) (from 12 to 13.5), the lubricant film thickness increases (from 2.125 to 6.203); (b) the lubricant film thickness increases (from 2.360 to 4.663) when μ (Pa·s) increases (from 0.01 to 0.04); and (c) increasing either r_5 or μ weakens the squeeze film effect on the lubricant film.

With reference to Figure 8(a) and Table 2, it is observed that at the moment of the pressure pulse, the leakage flow rate of the slipper-swashplate interface decreases (from 5.021 L/min to 1.834 L/min) when the r_2 (mm) increases

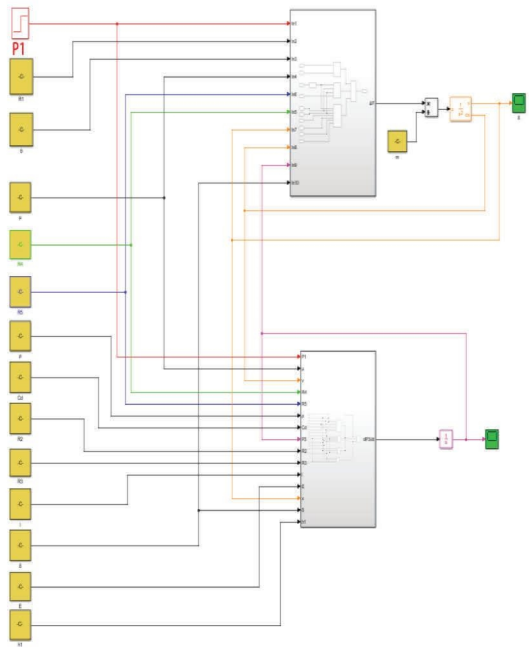

Figure 5: Simulink model of the squeeze film effect.

Table 1: Initial parametric values used in the nonlinear model.

Parameters	Values
r_1 (mm)	10
r_2 (mm)	1
r_3 (mm)	0.4
r_4 (mm)	6.5
r_5 (mm)	13
h_1 (mm)	1
μ (Pa·s)	0.028
l (mm)	19
h_0 (μm)	26

(from 0.6 to 1.2). However, in the end, the leakage flow rate will become the lowest when r_2 is the smallest. From Figure 8(b) and Table 2, there is a gradual decline in the leakage flow rate due to the decreases of r_3. The radius of the piston orifice and radius of the slipper orifice have opposite effects on the slipper leakage flow rate. For Figures 8(c) and 8(e) and Table 2, the width of the sealing land and the oil viscosity have the same tendency to affect the slipper leakage flow rate. All those trends in leakage are similar to Figure 8(a). As shown in Figure 8(d) and Table 2, the height of the slipper pocket and the radius of the slipper orifice have the same tendency to affect the leakage of the slipper pair.

From Figures 6 to 8, in the process of squeezing the lubricant film, both geometric parameters and working condition parameters affect the pressure buildup in the slipper pocket. Under the action of the pressure pulse, the leakage flow rate and oil film thickness are mainly affected by the establishment of slipper pocket pressure. The establishment of the slipper pocket pressure determines the support force buildup between the slipper and swashplate. When the time required to establish the support force becomes longer, the lubricant film will be quickly squeezed and thinned because of the squeeze film effect. At the same time, the leakage flow rate caused by the squeeze film effect will increase. After the slipper pocket pressure is built up, squeeze film speed becomes slower, and then the leakage flow rate is related to the lubricant film thickness at the next time. The smaller the film thickness is, the smaller the leakage is. Although the squeeze film effect leads to slipper leakage flow rate, which ultimately causes power loss, it shows that the establishment of the lubricating oil film between the slipper and swashplate ensures the proper action of the piston/slipper assembly under pressure pulse from the piston chamber at the moment.

4. Fluid Simulation of the Squeeze Film Effect

In this section, the Integrated Computer Engineering and Manufacturing Code for Computational Fluid Dynamics (ICEMCFD) is used to verify the squeeze film effect of the slipper pair. All the simulations are conducted using the commercial software package ANSYS 19.0, in which the ICEMCFD analysis module is used to calculate the squeeze process of the lubricant film of the slipper. A 3D CAD model of the lubricant film is created by the SolidWorks software, and then the model is imported into the ANSYS ICEMCFD. The model contains geometric parameters such as the inner and outer radius of the slipper sealing land and the assumed initial thickness of the slipper pads lubricant film. Also, the structure includes two surfaces of the lubricant film between the slipper and swashplate. The finite element model of

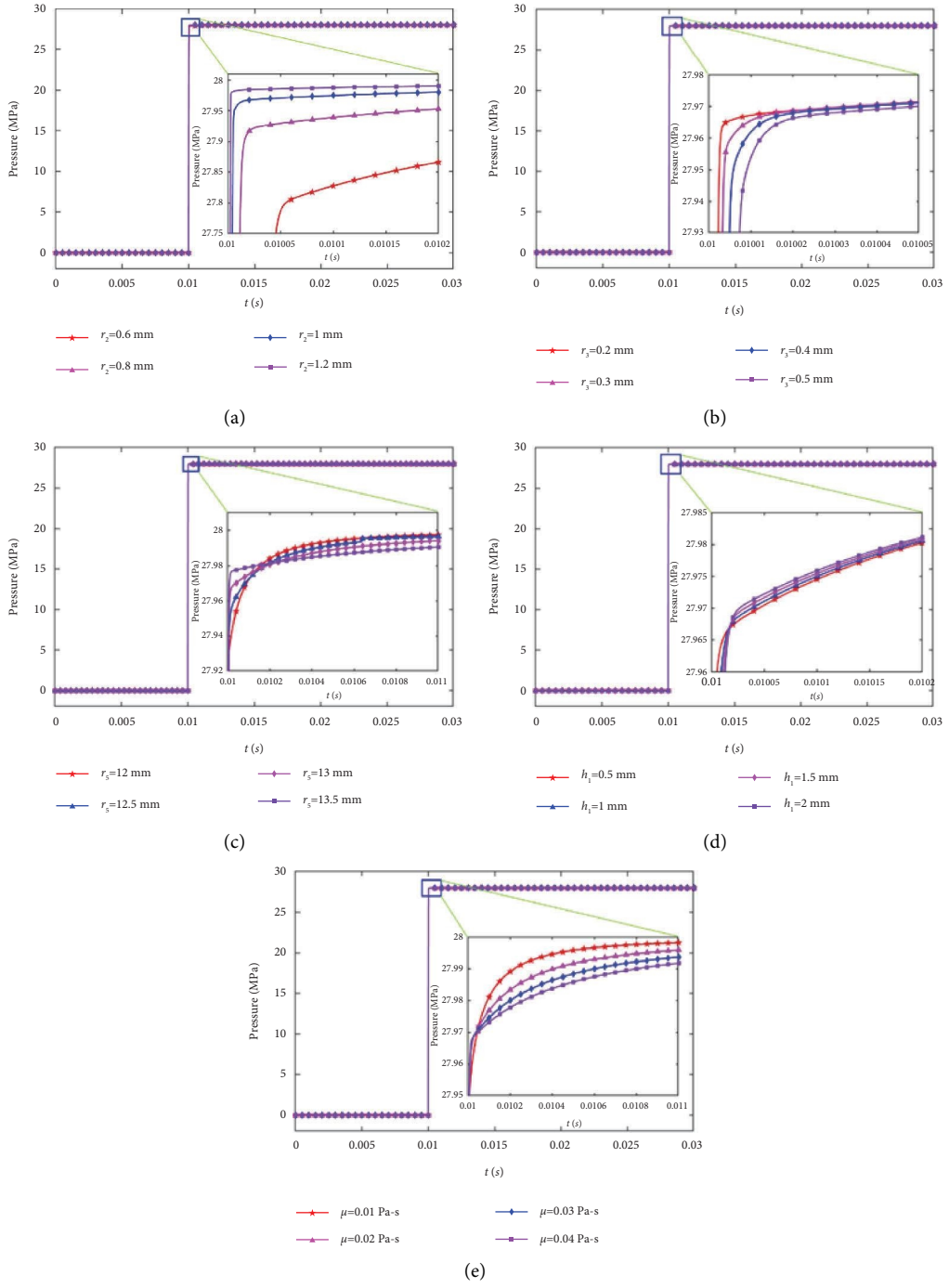

Figure 6: Slipper pocket pressure at different parameters: r_2 (a), r_3 (b), r_5 (c), h_1 (d), and μ (e).

Table 2: Variation of parameters under the squeeze film effect.

Parameter (range of change)	p_3 (MPa)	t (s)	h (μm)	Q (L/min)
r_2 (mm) (0.6~1.2)	27.81~27.98	6×10^{-5}~5×10^{-6}	3.903~3.922	5.021~1.834
r_3 (mm) (0.2~0.5)	27.969~27.965	3×10^{-6}~8×10^{-6}	3.921~3.919	1.606~2.962
r_3 (mm) (12~13.5)	27.99~27.98	5×10^{-4}~2×10^{-5}	2.125~6.203	2.804~2.357
h_1 (mm) (0.5~2)	27.97~27.975	1×10^{-5}~2×10^{-5}	3.921~3.917	1.893~3.279
μ (Pa·s) (0.01~0.04)	27.99~27.97	2×10^{-4}~1×10^{-5}	2.360~4.663	4.408~2.065

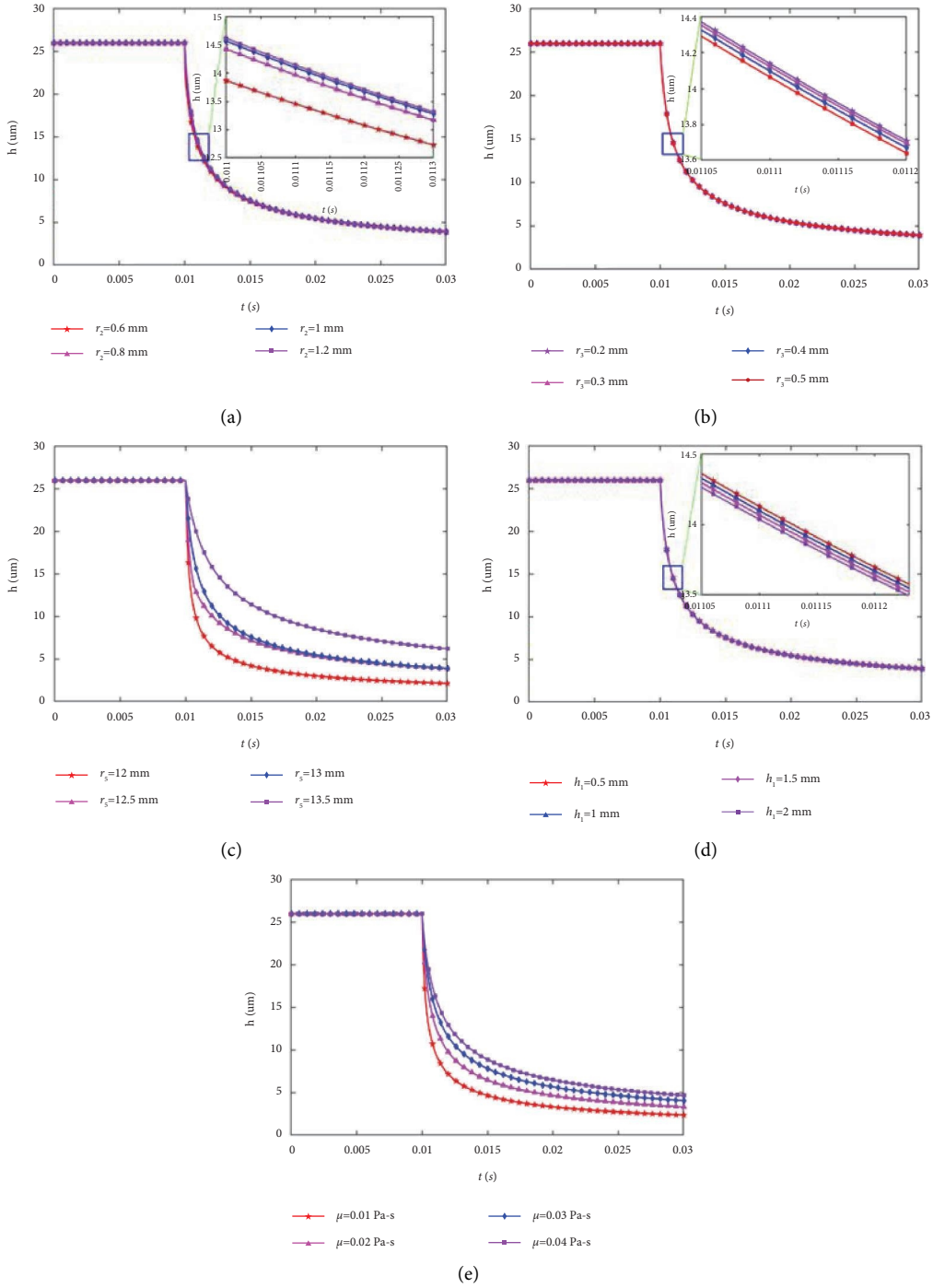

Figure 7: Thickness of the lubricant film at different r_2 (a), r_3 (b) r_5 (c), h_1 (d), and μ (e).

lubricant film is built up, which can efficiently and accurately perform finite element simulation of the squeeze film effect. Mesh delineation and generation are important in ANSYS fluid modal analysis, and the mesh quality determines the efficiency and accuracy of the model calculation. The Hex Dominant method is chosen to generate the mesh. And the meshing model of the lubricant film is shown in Figure 9.

In the fluid simulation, the slipper surface moved towards the swashplate surface. At the same time, pressure from the piston chamber acted on the oil film of the slipper. The thickness and pressure distribution field of the lubricant film were calculated and analyzed in Fluent. Figures 10 and 11 show the pressure distribution of the lubricant film between the slipper and swashplate at different squeeze speeds. The squeeze film speed is taken as 600 μm/s, 800 μm/s, 1000 μm/s, and 1200 μm/s, respectively, and consider the initial thickness of the lubricant film as 26 μm. Figure 12 focuses on the pressure distribution of the squeeze film

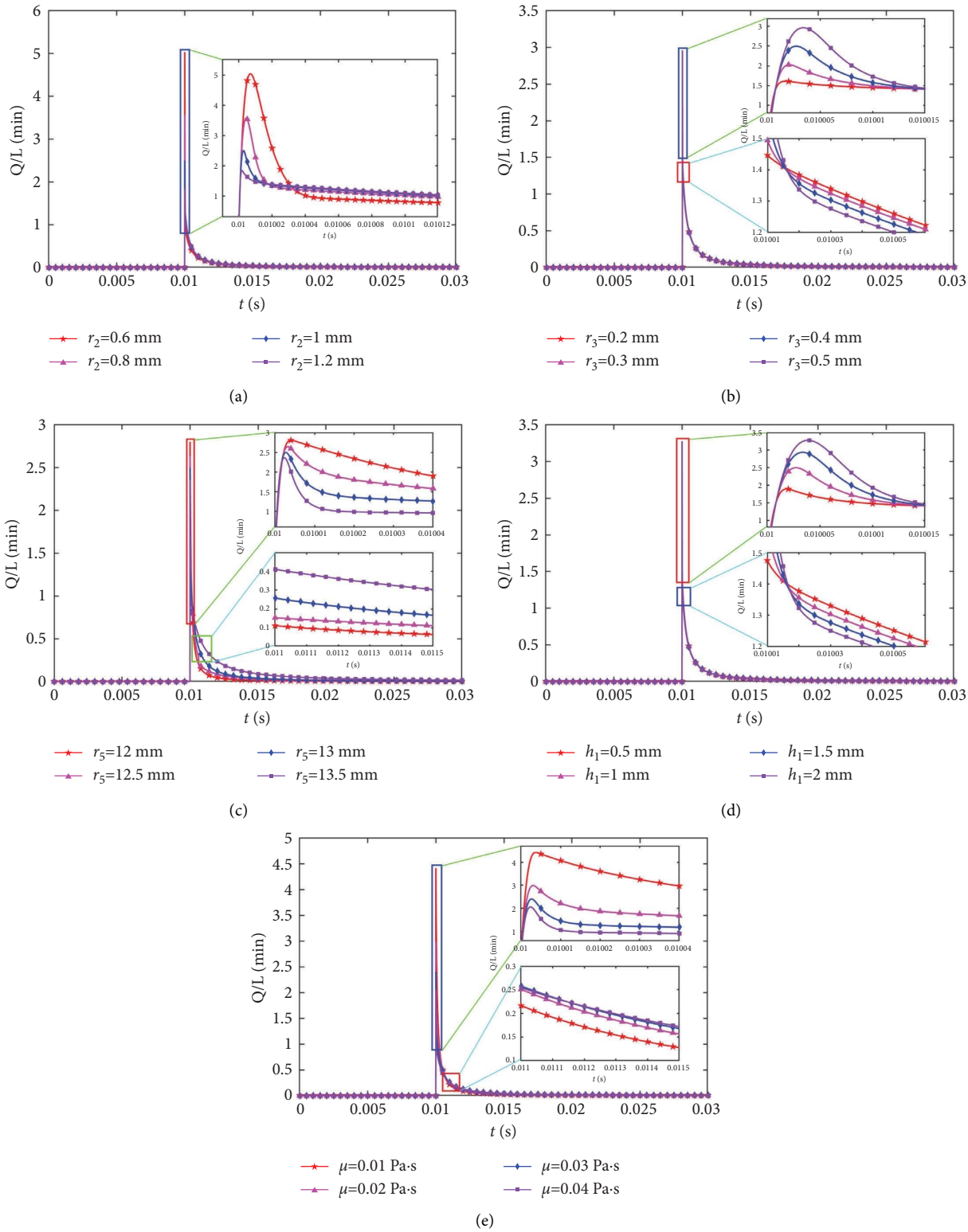

FIGURE 8: The slipper leakage flow rate at different r_2 (a), r_3 (b), r_5 (c), h_1 (d), and μ (e).

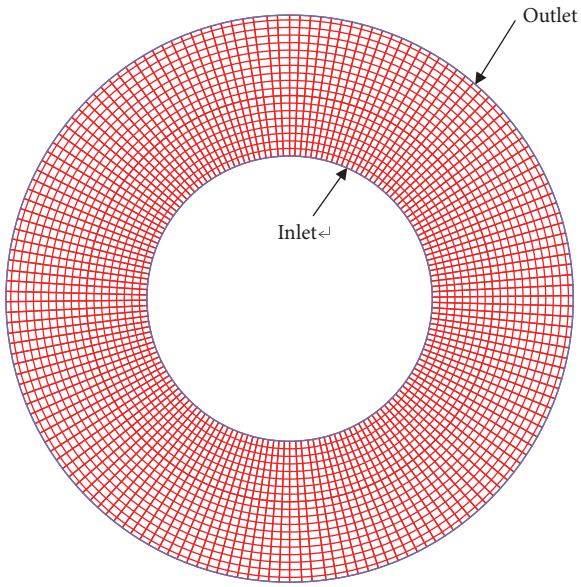

Figure 9: Lubricant film meshing model.

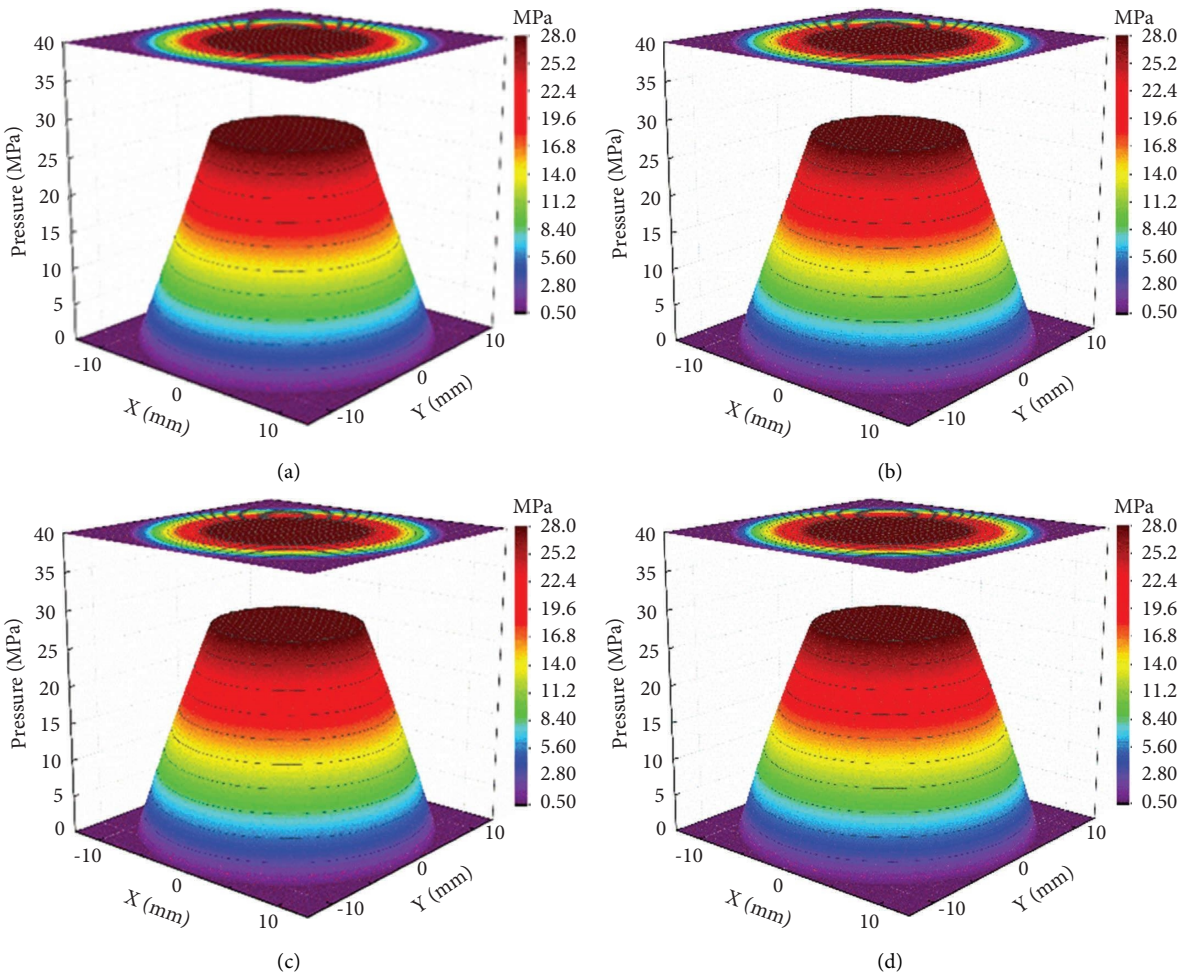

Figure 10: The pressure distribution of the oil film is different at different squeeze speeds. (a) $v = 600\ \mu$m/s. (b) $v = 800\ \mu$m/s. (c) $v = 1000\ \mu$m/s. (d) $v = 1200\ \mu$m/s.

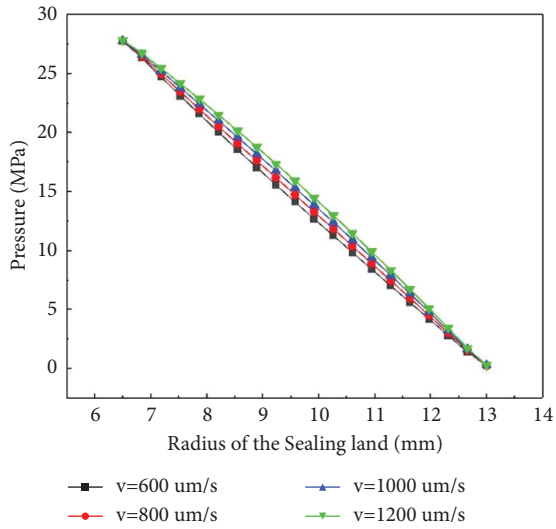

Figure 11: This expresses exactly the trend of pressure variation at different squeeze speeds.

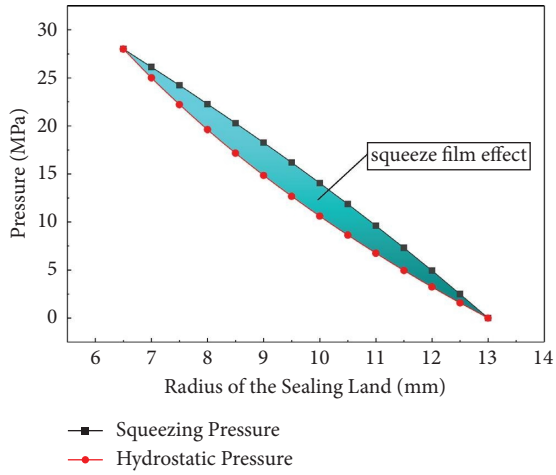

Figure 12: Squeeze film effect on the pressure distribution.

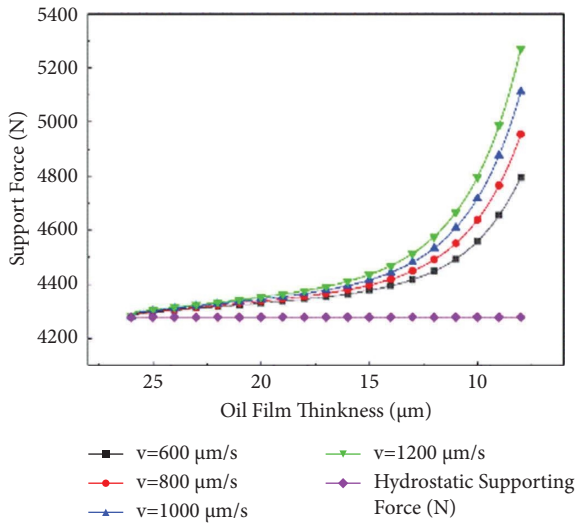

Figure 13: Support force for the piston/slipper assembly of the lubricant film.

effect. The presence of the squeeze film effect causes a change in the pressure distribution of the lubricant film.

Figure 13 illustrates the support forces for the piston/slipper assembly generated by the squeeze film effect. The higher squeeze speed corresponds to a higher support force, and the result is due to factor that the film thickness becomes lower due to the squeeze film effect. And the hydrostatic support force remains unchanged because the squeeze film effect has no effect on it.

5. Conclusion

In this paper, the squeeze film effect on the slipper pair is introduced. The mathematical model for the squeeze film effect is derived, in which varying structural parameters of the slipper/piston assembly and oil viscosity have an impact on the lubricant film's performance. The calculations and simulations on the lubricant film between the slipper and the swashplate with different parameters are achieved and different pressure distribution and support forces on the sealing land with varying squeeze velocity are obtained. The reasons for these results are analyzed. And from the mathematical modeling and simulation analysis, we can get

(1) The dynamic performance of the lubricant film is influenced by the squeeze film effect. Changes in geometric parameters affect the buildup of slipper pocket pressure, which in turn influences the squeeze film effect. The piston orifice and the slipper orifice have opposite effects on the lubricant film thickness and the amount of leakage flow. An increase in the radius of the piston orifice or the width of the sealing land leads to a reduction in squeeze leakage and an increase in the lubricant film thickness under squeeze film effect. The increase of the slipper pocket volume, slipper orifice radius, or oil viscosity makes the squeeze leakage increase and the oil film thickness decrease.

(2) An increase in the squeeze film speed will increase the load-bearing capacity of the lubricant film. The squeeze film effect can produce a higher support force, but an increase in the squeeze speed leads to a decrease in the oil film thickness and an increase of the lubricant film leakage flow. These results are encouraging for the high-speed design of piston pumps.

Nomenclature

p_1: Piston chamber pressure (MPa)
p_2: Slipper socket pressure (MPa)
p_3: Slipper pocket pressure (MPa)
p_4: Slipper sealing land pressure (MPa)
p_5: Pump chamber pressure (MPa)
F_p: Hydraulic force (N)
F_k: Spring force (N)
F_a: Inertia force (N)
F_f: Friction force (N)
F_{N1}: Hydrostatic support force (N)

F_{N2}: Squeeze support force (N)
θ: Swashplate angle (°)
m: Piston/slipper assembly mass (kg)
a: Piston/slipper assembly acceleration (m/s^2)
r_1: Piston radius (mm)
r_2: Piston orifice radius (mm)
r_3: Slipper orifice radius (mm)
r_4: Slipper sealing land inner radius (mm)
r_5: Slipper sealing land outer radius (mm)
r: Radius of any point on slipper sealing land (mm)
h: Slipper oil film thickness (mm)
μ: Oil viscosity (Pa · s)
l: Piston orifice length (mm)
C_d: Flow rate coefficient
ρ: Oil density (kg/m^3)
E: Volume oil elastic modulus (MPa)
V_1: Slipper pocket volume (m^3)
h_1: Slipper pocket height (mm)
h_0: Initial oil film thickness (mm).

Data Availability

The data used to support the finding of this study are included within the article.

Conflicts of Interest

The authors declare that they have no conflicts of interest.

Acknowledgments

This work was supported by a grant from the Shanxi Major Science and Technology Projects (grant no. 20191102009).

References

[1] F. Canbulut, "The experimental analyses of the effects of the geometric and working parameters on the circular hydrostatic thrust bearings," *The Japan Society of Mechanical Engineers*, vol. 48, no. 4, pp. 715–722, 2005.

[2] R. M. Harris, K. A. Edge, and D. G. Tilley, "Predicting the behavior of slipper pads in swashplate-type axial piston pumps," *Journal of Dynamic Systems, Measurement, and Control*, vol. 118, pp. 41–47, 1996.

[3] M. Deeken, *Displacement Units Simulation in DSHplus*, Olhydraulik und Pneumatik, Anaheim, CA, USA, 2001.

[4] M. Deeken, "Simulation of the reversing effects of axial piston pumps using conventional CAE tools," *Olhydraulik und Pneumatik*, vol. 46, 2002.

[5] M. Deeken, "Simulation of the tribological contacts in an axial piston machine," in *Proceedings of the Asme International Mechanical Engineering*, pp. 71–75, Anaheim, CA, USA, November 2004.

[6] N. D. Manring, C. L. Wray, and Z. Dong, "Experimental studies on the performance of slipper bearings within axial-piston pumps," *Journal of Tribology - Transactions of the ASME*, vol. 126, no. 3, pp. 511–518, 2004.

[7] M. Borghi, E. Specchia, and B. Zardin, "The critical speed of slipper bearings in axial piston swash plate type pumps and motors," in *Proceedings of the ASME 2009 Dynamic Systems and Control Conference*, Louis, MO, USA, June 2009.

[8] C.-J. Hooke and K.-Y. Li, "The lubrication of slippers in axial piston pumps and motors--the effect of tilting couples," *Proceedings of the Institution of Mechanical Engineers - Part C: Journal of Mechanical Engineering Science*, vol. 203, no. 5, pp. 343–350, 1989.

[9] C.-J. Hooke and Y.-P. Kakoullis, "Effects of centrifugal load and ball friction on the lubrication of slippers in axial piston pumps," *Intern fluid Power Symp*, vol. 6, 1981.

[10] M. Ivantysynova and C. Huang, "Thermal analysis in axial piston machines using CASPAR (simulation tool for performance prediction and design optimization) hangzhou," in *Proceedings of the Sixth International Conference on Fluid Power Transmission and Control*, Purdue University, West Lafayette, Indiana, March 2005.

[11] A. Schenk, "Predicting lubrication performance between the slipper and swashplate in axial piston hydraulic machines," *Dissertation for the Doctoral Degree*, pp. 23–30, Purdue University, West Lafayette, Indiana, 2014.

[12] J. Zhang, Q. Chao, and Q. Wang, "Experimental investigations of the slipper spin in an axial piston pump," *Measurement*, vol. 102, no. 5, pp. 112–120, 2017.

[13] Q. Chao, J. Zhang, B. Xu, and Q. Wang, "Multi-position measurement of oil film thickness within the slipper bearing in axial piston pumps," *Measurement*, vol. 122, pp. 66–72, 2018.

[14] N. B. Naduvinamani, P. S. Hiremath, and G. Gurubasavaraj, "Effect of surface roughness on the couple-stress squeeze film between a sphere and a flat plate," *Tribology International*, vol. 38, no. 5, pp. 451–458, 2004.

[15] M. Qing-rui and Y. Hou, "Effect of oil film squeezing on hydro-viscous drive speed regulating start," *Tribology International*, vol. 43, no. 11, pp. 2134–2138, 2010.

[16] N. M. Bujurke, N. B. Naduvinamani, and D. P. Basti, "Effect of surface roughness on magnetohydrodynamic squeeze film characteristics between finite rectangular plates," *Tribology International*, vol. 44, no. 7, pp. 916–921, 2011.

[17] A. Walicka, "Pressure distribution in a squeeze film of a Shulman fluid between porous surfaces of revolution," *International Journal of Engineering Science*, vol. 69, no. 5, pp. 33–48, 2013.

[18] G. Haidak and D. Wang, "Analysis of damage and failure mechanism under a lubricated slipper/swashplate interface in axial piston machines," *Procedia Structural Integrity*, vol. 35, pp. 124–131, 2022.

[19] S. Ye, H. Tang, Y. Ren, and J. Xiang, "Study on the load-carrying capacity of surface textured slipper bearing of axial piston pump," *Applied Mathematical Modelling*, vol. 77, no. 1, pp. 554–584, 2020.

[20] H. Tang, Y. Ren, and J. Xiang, "A novel model for predicting thermoelastohydrodynamic lubrication characteristics of slipper pair in axial piston pump," *International Journal of Mechanical Sciences*, vol. 124–125, pp. 109–121, 2017.

[21] S. Hashemi, A. Kroker, L. Bobach, and D. Bartel, "Multibody dynamics of pivot slipper pad thrust bearing in axial piston machines incorporating thermal elastohydrodynamics and mixed lubrication model," *Tribology International*, vol. 96, pp. 57–76, 2016.

[22] Y. Xu, *Oil Film Theory and Design of Friction Pairs for Hydraulic Pumps and Motors*, Machine Press, Beijing, China, 1987.